Electronic Supplementary Material (ESI) for Chemical Science.

Supporting Information

Development of fluorogenic substrates for colorectal tumor-related neuropeptidases for activity-based diagnosis

Norimichi Nagano, Yuki Ichihashi, Toru Komatsu,* Hiroyuki Matsuzaki, Keisuke Hata, Toshiaki Watanabe, Yoshihiro Misawa, Misa Suzuki, Shingo Sakamoto, Yu Kagami, Ayumi Kashiro, Keiko Takeuchi, Yukihide Kanemitsu, Hiroki Ochiai, Rikiya Watanabe, Kazufumi Honda, and Yasuteru Urano*

*Corresponding author. E-mail: T. K. (komatsu@g.ecc.u-tokyo.ac.jp),
Y. U. (uranokun@m.u-tokyo.ac.jp)

Table of Contents

Resources

Reagents	Source	Identifier
Biological samples		
Neurolysin, human recombinant	R&D Systems	Cat. #3814-ZN Lot #PPY0421101
THOP1, human recombinant	R&D Systems	Cat. #3439-ZN Lot #xPDL0121081
Bovine serum albumin	Wako	Cat. #016-15091 Lot #LEQ2235
Human serum	Aldrich	Cat. #H4522
Cells		
HT-29 cells	ATCC	Cat. #HTB-38
Kit		
CelLytic M	Sigma-Aldrich	Cat. #C2978
Bio-Rad protein assay dye reagent concentrate	Bio-Rad	Cat. #5000006JA

Experimental

General materials

All chemicals used were of analytical grade and were purchased from Tokyo Chemical Industries, Wako Pure Chemical Industries, Watanabe Chemical Industries, or Merck. Recombinant neurolysin and THOP1 were purchased from R&D Systems, Inc. (USA).

LC-MS analysis

LC-MS analysis was performed on an Acquity UPLC H-Class system (Waters) equipped with an Acquity UPLC BEH C18 1.7 μm (2.1 × 50 mm) column (Waters) and an MS detector (QDa or Xevo TQD, Waters).

UV-visible absorption and fluorescence spectroscopy

UV-visible spectra were obtained using a UV spectrometer (UV-1850, Shimadzu). Fluorescence analysis was performed using a fluorometric spectrometer (F-7100; Hitachi). The slit width was 5.0 nm for both the excitation and emission. The photomultiplier voltage is 400 V.

LC-MS based peptide metabolism study in assay of recombinant neurolysin (NLN)

20 μM synthetic peptide in Dulbecco's PBS (DPBS, pH 7.4) 30 μL and recombinant neurolysin (0.72 μg/mL) in DPBS 30 μL were mixed, and incubated at 37 °C for 1.5 h. For control condition, the

reaction was quenched without any incubation. Then, 30 μL 10 % formic acid in MeCN was added for quenching the reaction. LC-MS analysis was performed and peptides were detected by MS scanning (*m/z* = 300‐1500).

Michaelis-Menten plot

Varied concentrations of peptides and recombinant neurolysin or THOP1 (1 μg/mL) were mixed in DPBS containing 0.1 % CHAPS, and incubated at room temperature for 1 h. The reaction was quenched by adding 4× volume of MeOH-0.1 % formic acid. LC-MS analysis was performed, and the reaction rate was calculated from the formation of C-terminal products with multi reaction monitoring (MRM) mode. For the reaction of LVVSTQTALA, formation of TALA was monitored (*m/z* = 375.3 > 86.1 and 203.2 in positive mode), and for the reaction of Apd-STQTALK(NBD), formation of TALK(NBD) was monitored (*m/z* = 595.3 > 86.1 and 147.2 in positive mode). The multi-parameter fitting to Michaelis-Menten equation was performed using KaleidaGraph software using the formula Y = m1*X/(m2+X); X = [S], Y = v, m1 = V_{max}, m2 = K_m (m1 and m2 were variables).

Fluorometric assay with microplate reader

20 μM Apd-STQTALK(NBD) in DPBS 10 μL and colorectal cancer cell lysate in DPBS 10 μL were mixed in 384-well plate, and incubated at 37°C. Fluorescence was monitored on microplate reader EnVision 2103 (Perkin Elmer) under appropriate filter condition.

Preparation of tumor samples of colorectal cancer specimen

Both tumor and non-tumor tissue samples were freshly collected from surgical specimens excised from 13 patients with colorectal cancer at The University of Tokyo Hospital[1]. Informed consent was obtained from all patients and the study was approved by the institutional ethics review board (review number 10177-(1)). The areas of cancerous and normal lesions were macroscopically distinct, and the final diagnosis of colorectal cancer was confirmed histopathologically in all cases. Both tumor and normal samples were labeled with randomly generated numbers, which were blinded to the examiners.

Plasma samples from healthy controls and patients with colorectal cancer

Plasma samples of colorectal cancer and healthy volunteer for validation study were obtained from P-EBED (The Platform for Evaluating Biomarkers of Cancer Early Detection). National Cancer Center Hospital (Tokyo, Japan) and Kagoshima Prefectural Comprehensive Health Center joined to P-EBED with supporting from P-CREATE of the Japan Agency for Medical Research and Development (AMED). Other

plasma samples used exploratory study were collected in Osaka National Hospital (Osaka, Japan), Osaka Medical College (Takatsuki Japan), with supporting from the Program for Promotion of Fundamental Studies in Health Sciences conducted by the National Institute of Biomedical Innovation of Japan, Health and Labour Sciences Research Grants from the Ministry of Health, Labor and Welfare of Japan[2,3]. Ethical approval for this study was obtained from the central ethics committees of Nippon Medical School (M-2021-002) and the ethical committee of Nippon Medical School (A-2020-032 and A-2020-044).

Preparation of microdevices for assay

Chamber array devices were prepared based on a previous report[4], with some modifications. In brief, a glass coverslip (24 mm × 32 mm) was immersed in 8 M KOH, sonicated for 90 min, and incubated overnight. The coverslip was then rinsed with pure water and dried using an air blow gun. It was spin-coated with an amorphous fluorocarbon polymer (9 % CYTOP; AGC, Japan) at 1000 rpm for 30 s, baked at 80 °C for 10 min, and then at 180 °C for 1 h on a hotplate. The thickness of the CYTOP layer was 1.6 μm. The CYTOP-coated coverslip was spin-coated with a positive photoresist (AZ P4620; AZ Electronic Materials, USA) at 7500 rpm for 30 s and baked at 100 °C for 5 min. After rehydration of the photoresist at 25 °C under 60 % humidity, photolithography was carried out using a photomask with 1.8 μm holes, separated by 8 μm, and then incubated for 90 s in a developer (AZ300 MIF, AZ Electronic Materials, USA). The resist-patterned coverslip was dry-etched with O_2 plasma using a reactive ion etching system (DES-101E; YAC, Japan, or RIE-10NR or PC-300; Samco, Japan) to remove the exposed CYTOP. The substrate was cleaned and rinsed with acetone, isopropanol, and pure water to remove the remaining photoresist. The resulting CYTOP-on-coverslip substrate contained an array of exposed SiO_2 patterns with a diameter of 3.2 μm.

Single-molecule enzyme assay of neuropeptidases in the microdevice

The enzyme stock solution was diluted with assay buffer (HEPES 100 mM, pH 7.4, $MgCl_2$ and $CaCl_2$ 1 mM, DTT 1 mM and Triton X-100 3 mM) at 25°C. containing fluorescence probes (Apd-STQTALK(NBD) 50 μM), and the mixture (15 μL) was introduced into the microdevice by manual pipetting. The device was placed on ice for 5 s and returned to room temperature. FC-70 (30 μL) (SIGMA-ALDRICH, Co., USA) was gradually introduced and exchanged with Fomblin PFPE (40 μL) (Solvay) to complete the sealing. The device was incubated at 37°C in a benchtop incubator (FCI-280, AS-ONE) for 4 h. Fluorescence images were acquired using an epifluorescence microscope (Ti2, Nikon) equipped with a 20× dry objective lens (Plan Apo 20×), sCMOS camera (ORCA-Fusion C14440, Hamamatsu photonics), white LED illumination unit (X-Cite Xylis, Opto Science), and a motorized stage. The assay was

performed using a solution containing sTM (10 μM) as an internal standard[5], and the focus was adjusted using its fluorescence. Images were acquired by tile scan mode with the perfect focus. The excitation and emission filters used were FITC (mirror = 510- nm, Ex. = 460-500 nm, Em. = 510-560 nm) and mCherry (mirror = 600- nm, Ex. = 550-590 nm, Em. = 608-683 nm), respectively.

Image processing

Images were processed using general analysis module of NIS-Elements AR version 5.30.00 (Nikon). Firstly, all fluorescence images were background corrected using rolling ball correction (3.25 μm). Then, we define the wells included in the analysis by monitoring the fluorescence of the loading control dye (sTM) monitored in mCherry channel; wells with sTM fluorescence were chosen by bright spot detection (3 μm), and irregular fluorescent spots from fluorescent debris or air bubbles that showed stronger sTM fluorescence or fluorescence spots at irregular positions were omitted by detecting them by bright spot detection and dilating the ROIs and removing the overlapping ROIs by size (fill area < 40) and shape (circularity > 0.7) filters. Then, regions of interest (ROIs) of the active enzymes were defined by bright spot detection in FITC channel (size 3 to 5 μm) with contrast threshold to omit the empty wells. The fluorescence signals were acquired as mean of signals from each ROI. Neurolysin signal ratio (%) was calculated by dividing the number of wells containing the active enzymes by that of all wells analyzed. The data were processed using Python, Excel or Kaleidagraph software to construct histograms and scattered plots.

Cell culture and preparation of lysates.

HT-29 cells were cultured in Dulbecco's Modified Eagle medium (DMEM medium (1×), Gibco 11885-084), supplemented with 10 % (v/v) fetal bovine serum, 1 % (v/v) Penicillin-Streptomycin (Gibco, 15410-122) in a humidified incubator under 5 % CO_2 in 95 % air. For preparation of cell lysates, cells cultured to 50-80 % confluency in 10 cm culture dish were washed twice with PBS (3 mL) and lysed with CelLytic M (500 μL) for 10 min at room temperature. Lysate was moved to 1.5 mL plastic tube, centrifuged (14,000 rpm × 10 min, 4 °C), and the supernatant was collected and fresh frozen in liquid N_2. Protein concentration was measured with Bradford reagent using BSA as a standard.

Supplementary data for preparation of compounds

Preparation of 3-aminopropyl-dabcyl (Apd)

p-Aminobenzoic acid (2.7 g, 19.7 mmol) was dissolved in 200 mL 0.1N HCl aq. on ice. Sodium nitrite (2.1 g, 30.0 mmol) dissolved in 10 mL H_2O was added in small portions, and the reaction was stirred for 20 min on ice. Aminosulfuric acid (1.9 g, 19.7 mmol) was added slowly, and the solution was neutralized with 50 mL sat. $NaHCO_3$ aq. *N*-(3-Aminopropyl)-*N*-methylaniline (2.6 mL, 15.8 mmol) was added dropwise, and the reaction was stirred for 1 h on ice. Red precipitate was filtered and washed twice with H_2O to afford Apd (3.5 g, y. 38 %) with > 80 % purity.

^{1}H-NMR (300 MHz, CD_3OD): δ 1.88 (m, 2H), 2.8-2.9 (m, 5H), 3.12 (m, 2H), 6.65 (d, 2H, *J* = 8.2 Hz), 6.71 (d, 2H, *J* = 8.2 Hz), 7.15 (d, 2H, *J* = 8.2 Hz), 7.74 (d, 2H, *J* = 8.2 Hz). HRMS (ESI$^+$): calcd. for $[M+H]^+$, 313.1665; found, 313.1675 (+ 1.0 mms).

Preparation of Fmoc-Apd-OH

Apd-OH (3.5 g, 11.2 mmol) was dissolved in 100 mL 1,4-dioxane and 100 mL H_2O, and sodium carbonate (3.5 g, 33.6 mmol) was added slowly. In this condition, Apd did not completely dissolve. To the mixture, Fmoc-Cl (2.9 g, 11.2 mmol) in 30 mL 1,4-dioxane was added dropwise, and the reaction was stirred at room temperature for 3 h, after which the remaining Apd completely dissolved. After the complete loss of the reactant was confirmed with UPLC-MS-based reaction monitoring, 1,4-Dioxane in solution was removed in vacuo, and the solution was acidified (to pH ~ 1) with 2N HCl aq. The dark red precipitate was filtered, and washed with H_2O twice to afford Fmoc-Apd-OH (5.2 g, y. 87 %) with > 95 % purity.

^{1}H-NMR (300 MHz, CD_3OD): δ 1.89 (m, 2H), 3.18 (m, 2H), 3.33 (s, 3H), 3.86 (t, 2H, *J* = 7.2 Hz), 4.18 (t, 1H, *J* = 7.2 Hz), 4.39 (d, 2H, *J* = 7.2 Hz), 7.13 (d, 2H, *J* = 8.8 Hz), 7.2-7.4 (m, 4H), 7.63 (d, 2H, *J* = 8.8 Hz), 7.7-7.8 (m, 4H), 7.92 (d, 2H, *J* = 8.8 Hz), 8.13 (d, 2H, *J* = 8.8 Hz).

HRMS (ESI$^+$): calcd. for $[M+H]^+$, 535.2345, found, 535.2354 (+ 0.9 mms).

Peptide synthesis

All peptides were synthesized on automatic peptide synthesizer (Syrol; Biotage) using standard protocols of fluorenylmethoxycarbonyl (Fmoc) solid-phase peptide synthesis (SPPS) with 2-chlorotrityl chloride resin (for model peptides and LVVSTQTALA-derived peptides) or rink amide resin (for YVVSTQTALA-NH_2). Fmoc-Apd was used as building block just like other Fmoc-amino acids. After the elongation of the peptides, resin beads were washed 2 times with 2 mL DCM, and peptides

were cleaved from the resin by incubating with 2.4 mL TFA/H_2O/Triethylsilane = 10/1/1 for 1 h. The solution was filtered, evaporated, and the resultant peptides were purified by HPLC under the following conditions: A/B = 90/10-40/60 (30 min) (solvent A: H_2O with 0.1 % TFA, solvent B: acetonitrile/H_2O (with 0.1 % TFA) = 80/20). The purity of the peptide was confirmed by LC-MS analysis under the following conditions: A/B = 100/0-0/100 (0.5 min isocratic, 3.5 min) (solvent A: H_2O with 0.1% formic acid, solvent B: acetonitrile with 0.1% formic acid). 280 nm absorbance was monitored.

YVVSTQTALA (ESI^-) *m/z* calcd. for $[M-H]^-$: 1050.54770, found: 1050.54535 (-2.35 mmu)

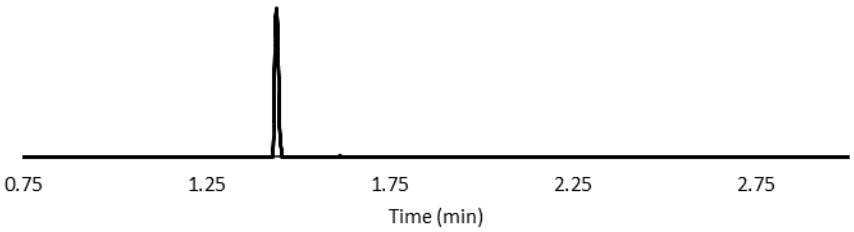

GGGYVVSTQTALA (ESI^-) *m/z* calcd. for $[M-H]^-$: 1221.61209, found: 1221.60908 (-3.01 mmu)

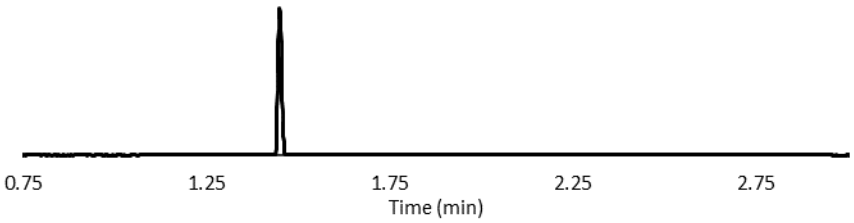

YVVSTQTALA-NH_2 (ESI^+) *m/z* calcd. for $[M+Na]^+$: 1073.56018, found: 1073.56066 (+0.48 mmu)

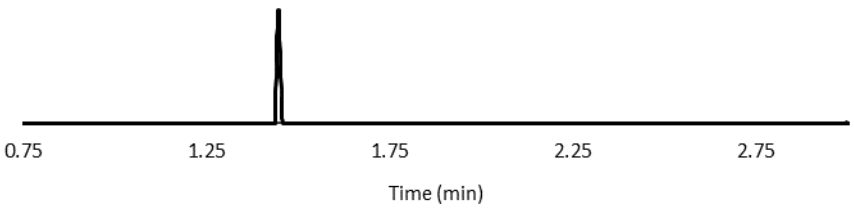

YVVSTQTALAGGG (ESI^-) *m/z* calcd. for $[M-H]^-$: 1221.61209, found: 1221.61179 (-0.30 mmu)

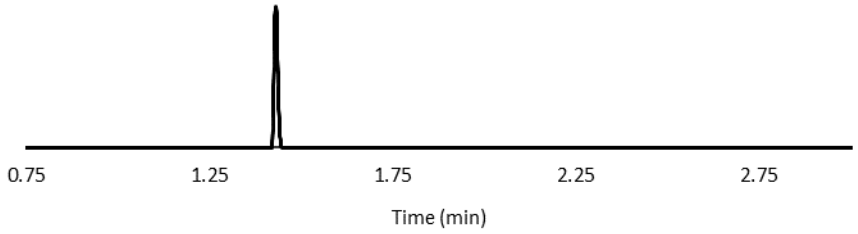

Apd-VVSTQTALA (ESI$^-$) *m/z* calcd. for $[M-2H]^{2-}$: 590.31258, found: 590.31456 (+1.98 mmu)

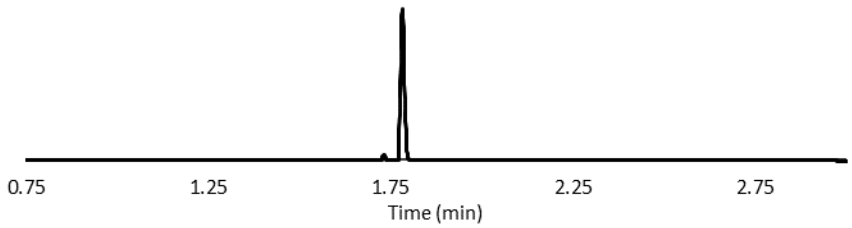

Apd-VSTQTALA (ESI$^-$) *m/z* calcd. for $[M-H]^-$: 1082.56402, found: 1082.56305 (-0.97 mmu)

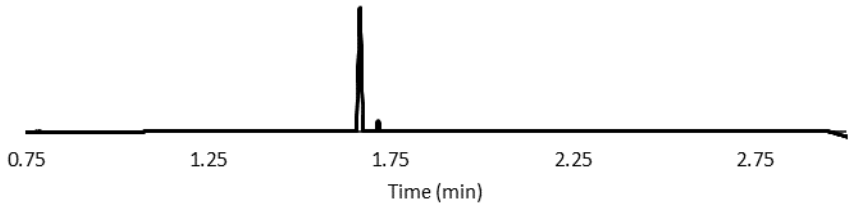

Apd-STQTALA (ESI$^-$) *m/z* calcd. for $[M-H]^-$: 983.49560, found: 983.9432 (-1.28 mmu)

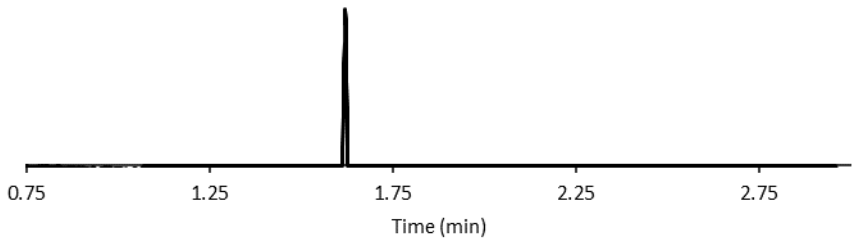

YVVSTQTALK (ESI$^+$) *m/z* calcd. for $[M+H]^+$: 1109.62010, found: 1109.61997 (-0.13 mmu)

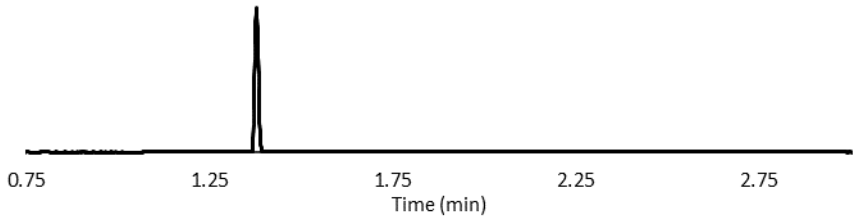

YVVSTQTALD (ESI$^-$) *m/z* calcd. for $[M-2H]^{2-}$: 546.76513, found: 546.76379 (-1.34 mmu)

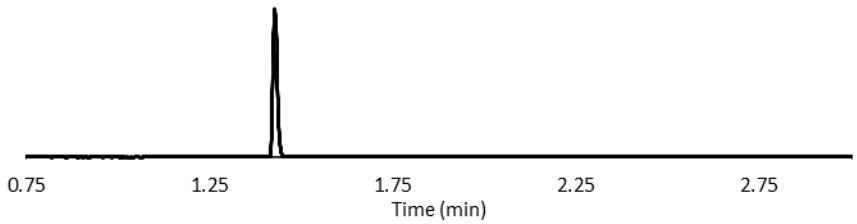

YVVSTQTALE (ESI$^-$) *m/z* calcd. for $[M-H]^-$: 1108.55318, found: 1108.55268 (-0.50 mmu)

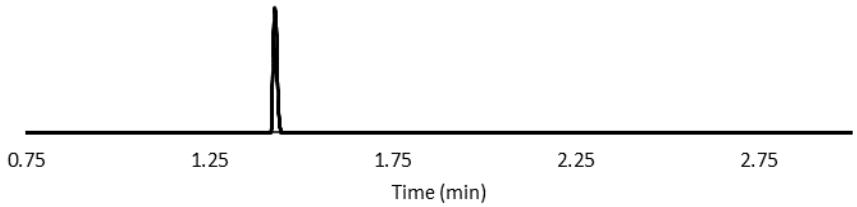

YVVSTQTALK(Cbz) (ESI$^-$) *m/z* calcd. for $[M-H]^-$: 1241.64233, found: 1241.64331 (+0.98 mmu)

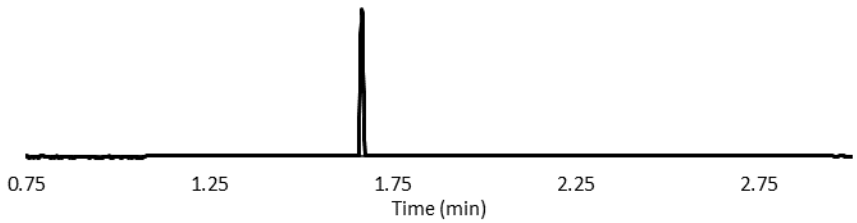

Acetylation of N-terminal amino group

Peptides were prepared by Fmoc-SPPS with 2-chlorotrityl chloride resin. After elongation of the peptide, to the resin were added DMF 400 μL, 2 M DIEA in NMP 400 μL and acetic anhydride 400 μL and shaken for 1.5 h. The subsequent procedures of washing resin were the same as peptide synthesis.

Ac-YVVSTQTALA (ESI$^-$) *m/z* calcd for $[M-H]^-$: 1092.55830, found: 1092.55798 (-0.32 mmu)

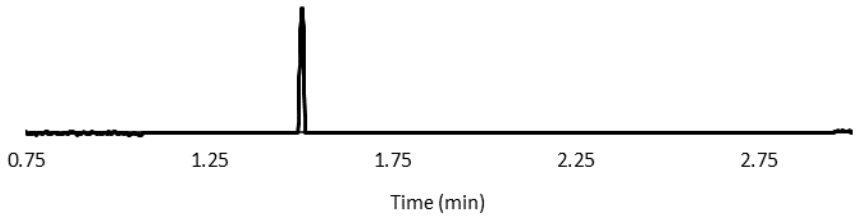

Condensation reaction between peptide amino group and fluorophore carboxyl group (FL and HCCA)

Peptides were prepared by Fmoc-SPPS with 2-chlorotrityl chloride resin. After elongation of the peptide, to the resin were added *N*-hydroxysuccinimidyl ester of 7-Hydroxycoumarin-3-carboxylic acid (HCCA-NHS) or *N*-hydroxysuccinimidyl ester of 6-carboxyfluorescein (FL-NHS) in DMF (2.5 eq to resin beads), and 2 M DIEA in NMP 400 μL and shaken for 2.5 h. The subsequent procedures of washing resin were the same as peptide synthesis.

FL-VVSTQTALA (ESI$^-$) *m/z* calcd. for $[M-2H]^{2-}$: 622.26242, found: 622.25913 (-3.29 mmu)

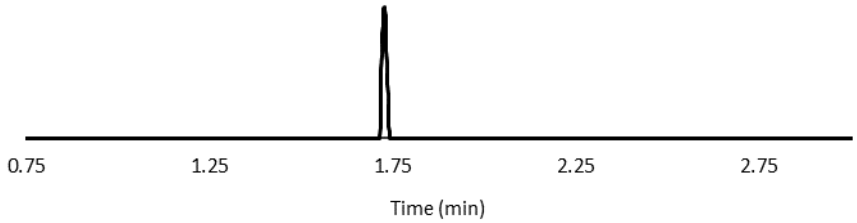

HCCA-VVSTQTALA (ESI$^-$) *m/z* calcd. for $[M-2H]^{2-}$: 537.24403, found: 537.24454 (+0.51 mmu)

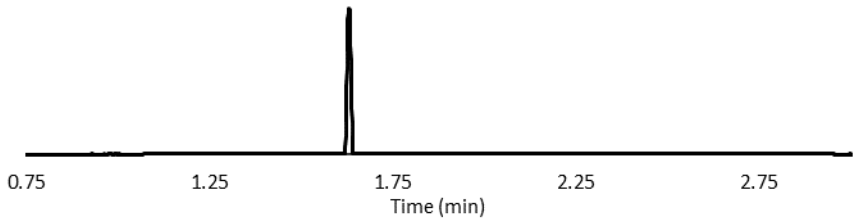

Synthesis of YVVSTQTALK(NBD), YVVSTQTALK(FL), and Apd-STQTALK(NBD)

Peptides were prepared by Fmoc-SPPS with 2-chlorotrityl chloride resin. After elongation of the peptide without the cleavage of deprotection of Fmoc at N terminus, the resin beads were washed 2 times with 2 mL DCM and cleaved by 1% TFA in DCM and a few drops of triethylsilane. Then, the solution was evaporated, and distillation was dissolved in DMSO 1 mL. After addition of 500 μL DIEA, FL-NHS or NBD-Cl was added. The solution was stirred for 2.5 h at r.t. Then, Piperidine 1 mL was added for deprotection. The solution was evaporated, and the compound was purified over HPLC under the following conditions: A/B = 90/10-40/60 (30 min) (solvent A: H_2O with 0.1 % TFA, solvent B: acetonitrile/H_2O (with 0.1 % TFA) = 80/20).

YVVSTQTALK(NBD) (ESI^-) *m/z* calcd. for $[M-2H]^{2-}$: 634.80003, found: 634.80098 (+0.95 mmu)

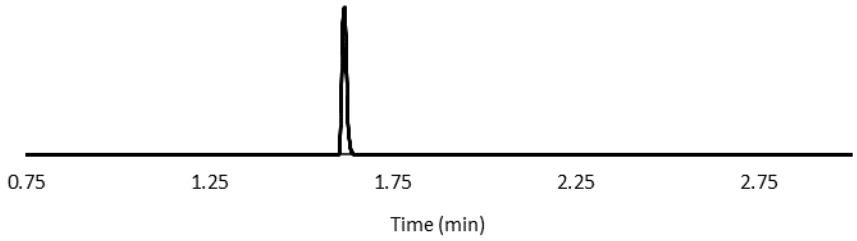

YVVSTQTALK(FL) (ESI^-) *m/z* calcd. for $[M-2H]^{2-}$: 732.32300, found: 732.32131 (-1.69 mmu)

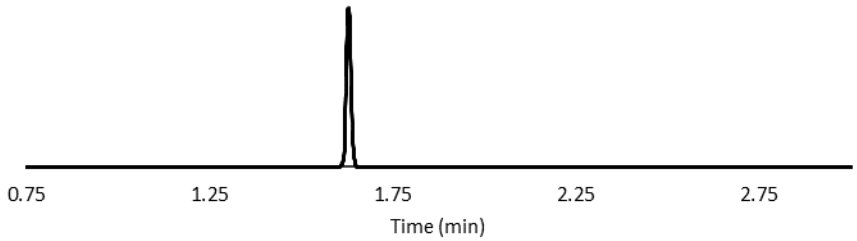

Apd-STQTALK(NBD) (ESI^-) *m/z* calcd. for $[M-H]^-$: 1203.55524, found: 1203.55248 (-2.76 mmu)

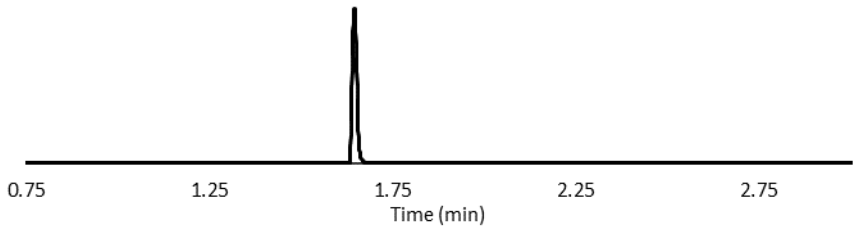

^{1}H-NMR (400 MHz, CD_3OD): δ 0.90 (d, 3H, *J* = 6.4 Hz), 0.94 (d, 3H, *J* = 6.4 Hz), 1.19 (d, 3H, *J* = 6.0 Hz), 1.27-1.33 (m, 15H), 1.40 (d, 3H, *J* = 7.3 Hz), 1.46-1.56 (m, 2H), 1.58-1.84 (m, 6H), 1.87-1.95 (m, 1H), 1.96-2.09 (m, 3H), 2.14-2.22 (m, 1H), 2.36 (t, 2H, *J* = 7.3 Hz), 3.02 (t, 2H, *J* = 7.8 Hz), 3.10

(s, 3H), 3.21 (q, 7H, *J* = 7.3 Hz), 3.60 (t, 2H, *J* = 7.1 Hz), 3.99-4.10 (m, 2H), 4.22-4.41 (m, 9H), 6.27 (d, 1H, *J* = 8.7 Hz), 6.83 (d, 2H, *J* = 9.2 Hz), 7.78-7.81 (m, 2H), 7.82-7.84 (m, 2H), 8.00-8.02 (m, 2H), 8.46 (d, 1H, *J* = 8.7 Hz). The compound was the salt with 1.1 equivalent of triethylamine.

Synthesis of TALK (NBD)

Peptides were prepared by Fmoc-SPPS with 2-chlorotrityl chloride resin. Lys whose εN was protected by 4-metoxytrityl group (Mmt) was used for the first elongation step. before deprotection of Fmoc, Mmt was deprotected by incubation with 2 mL TFA/H_2O/Triethylsilane = 1/50/1 for 10 min. Then, resin beads were washed 2 times with 2 mL DCM, and incubated with NBD-Cl in DMF (2.5 eq to resin beads), and 2 M DIEA in NMP 400 μL for 2.5 hr. After elongation of the peptide, the resin beads were washed 2 times with 2 mL DCM. After the cleavage, the compound was purified over HPLC under the following conditions: A/B = 90/10-40/60 (30 min) (solvent A: H_2O with 0.1 % TFA, solvent B: acetonitrile/H_2O (with 0.1 % TFA) = 80/20).

TALK(NBD) (ESI^-) *m/z* calcd. for $[M-H]^-$: 593.26890, found: 593.26602 (-2.88 mmu)

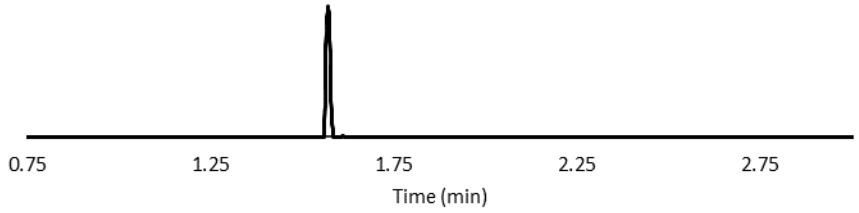

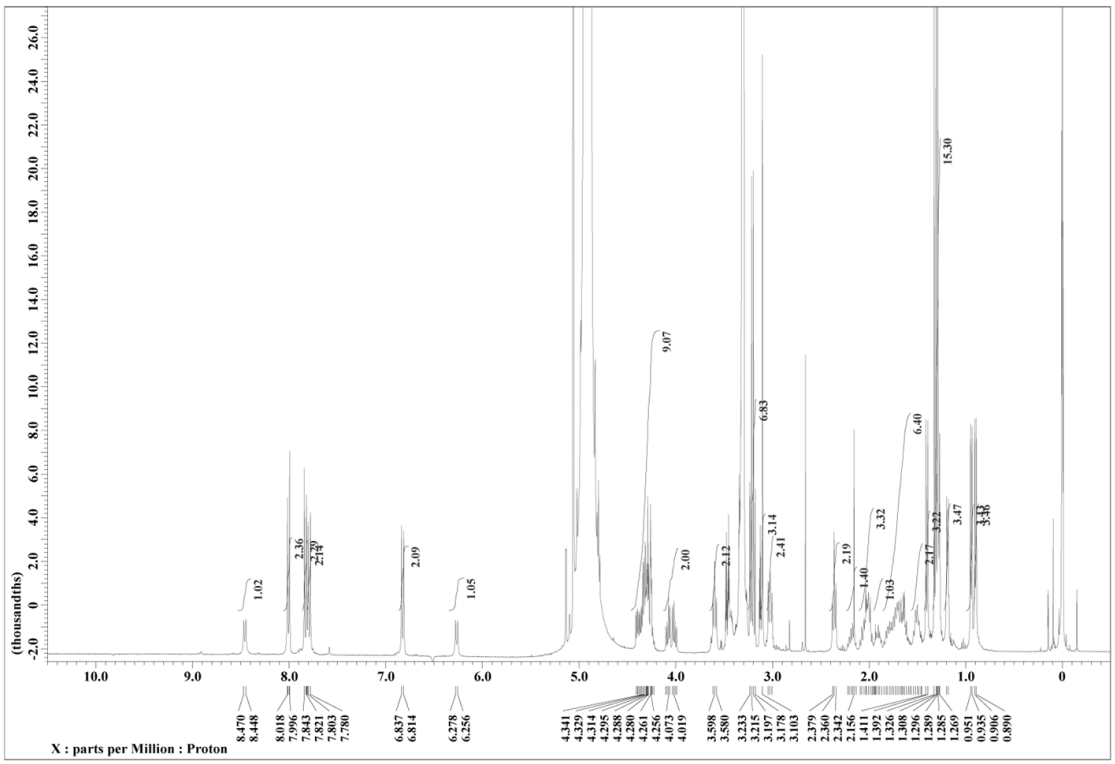

^{1}H-NMR spectra of Apd-STQTALK(NBD)

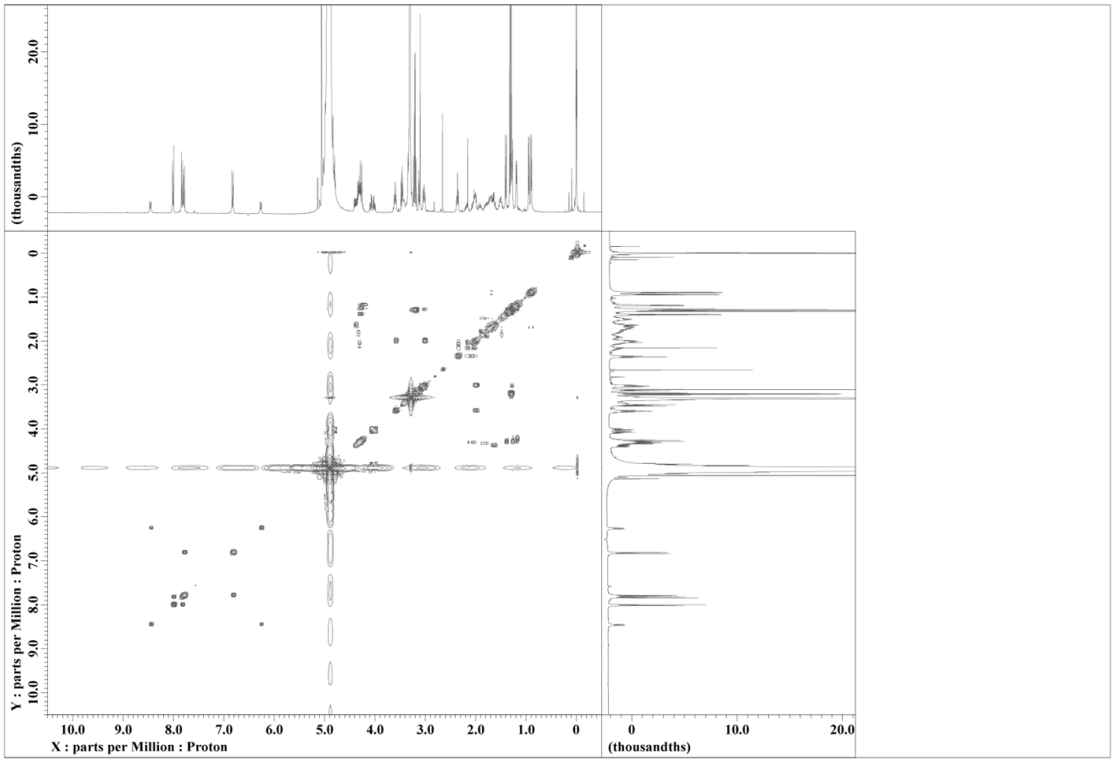

COSY spectra (full)

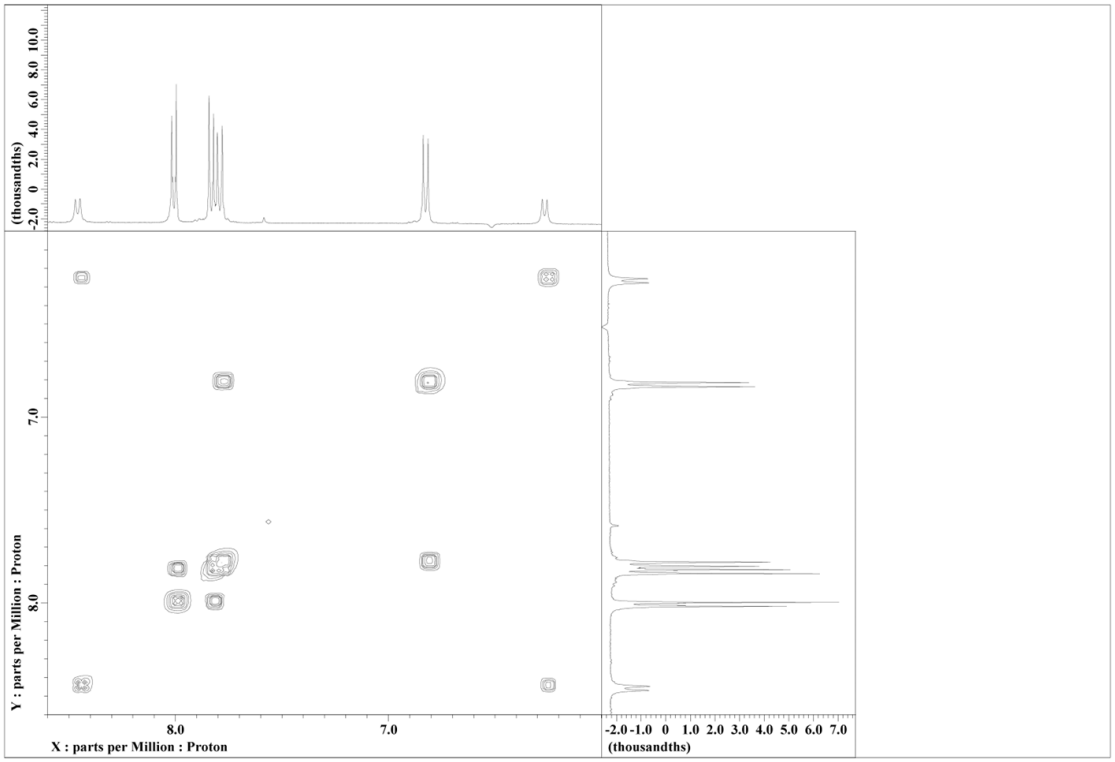

COSY spectra (high magnetic field)

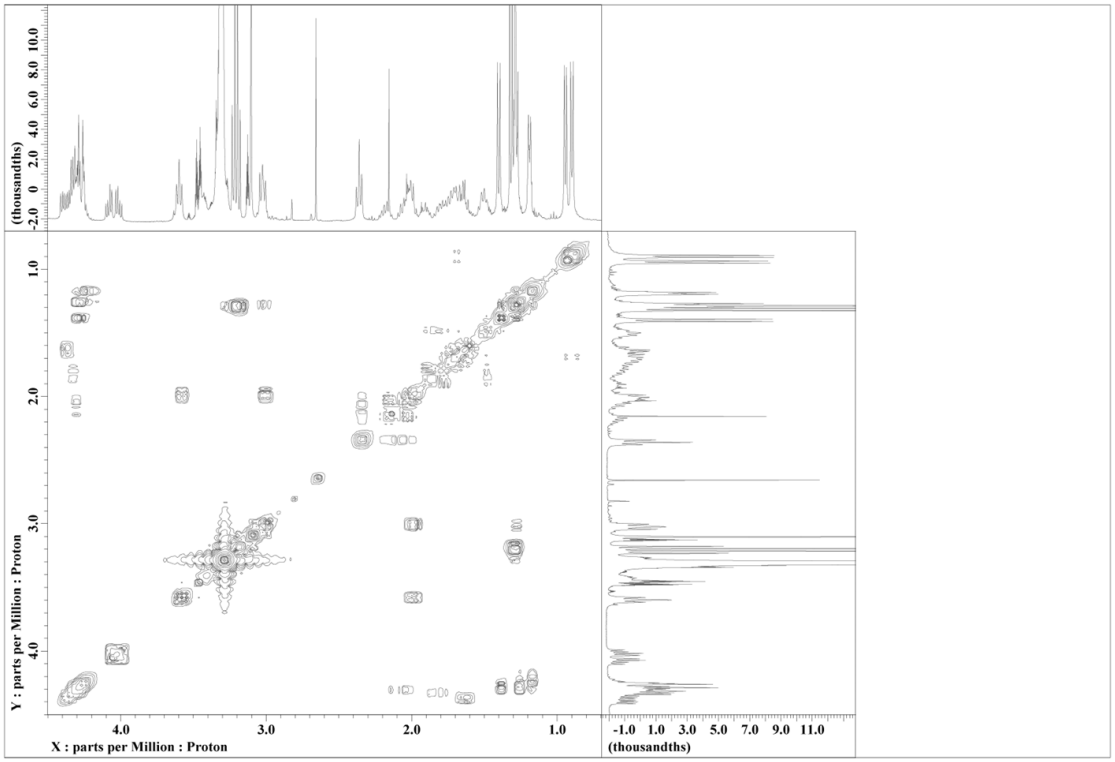

COSY spectra (low magnetic field)

Supplementary Tables

Table S1. Summarized information about the plasma samples

Category		Healthy controls	Pancreatic tumor	Gastric tumor	Colorectal tumor
Sample number		30	13	12	28
Stage	I	-	2	4	4
	II	-	5	2	11
	III	-	1	3	8
	IV	-	5	3	5
Age (mean ± S.D.) years old		36.6 ± 11.5	71.3 ± 8.0	68.6 ± 8.6	66.5 ± 8.0
Gender (female/male)		16/14	7/6	11/1	17/11

Table S2. Summarized information about the plasma samples used in the second set of experiments.

Category		Healthy controls	Colorectal tumor
Sample number		30	27
Stage	I	-	9
	II	-	11
	III	-	6
	IV	-	1

Table S3. Summarized information about neurolysin signal ratio values for each patient with colorectal tumor and healthy control.

#	*Label*	*Stage*	*Neurolysin signal ratio (%)*
1	Colorectal tumor	IV	0.094
2	Colorectal tumor	II	0.180
3	Colorectal tumor	II	0.054
4	Colorectal tumor	II	0.056
5	Colorectal tumor	III	0.081
6	Colorectal tumor	IV	0.782
7	Colorectal tumor	II	0.054
8	Colorectal tumor	I	0.176
9	Colorectal tumor	II	0.189
10	Colorectal tumor	II	0.106
11	Colorectal tumor	II	0.897
12	Colorectal tumor	III	0.395
13	Colorectal tumor	IV	0.044
14	Colorectal tumor	I	0.065
15	Colorectal tumor	III	0.040
16	Colorectal tumor	IV	0.107
17	Colorectal tumor	IV	0.157
18	Colorectal tumor	I	0.071
19	Colorectal tumor	III	0.117
20	Colorectal tumor	II	0.408
21	Colorectal tumor	III	0.052
22	Colorectal tumor	III B	0.088
23	Colorectal tumor	I	0.035
24	Colorectal tumor	II	0.131
25	Colorectal tumor	III	0.015
26	Colorectal tumor	III	0.187
27	Colorectal tumor	II	0.078
28	Colorectal tumor	II	0.028
29	Healthy	-	0.140
30	Healthy	-	0.030
31	Healthy	-	0.017
32	Healthy	-	0.060
33	Healthy	-	0.045
34	Healthy	-	0.019
35	Healthy	-	0.031
36	Healthy	-	0.044
37	Healthy	-	0.026
38	Healthy	-	0.038
39	Healthy	-	0.049
40	Healthy	-	0.216
41	Healthy	-	0.146
42	Healthy	-	0.170
43	Healthy	-	0.181
44	Healthy	-	0.071
45	Healthy	-	0.040
46	Healthy	-	0.075
47	Healthy	-	0.025
48	Healthy	-	0.023
49	Healthy	-	0.052
50	Healthy	-	0.052
51	Healthy	-	0.023
52	Healthy	-	0.216
53	Healthy	-	0.034
54	Healthy	-	0.042
55	Healthy	-	0.030
56	Healthy	-	0.008
57	Healthy	-	0.032
58	Healthy	-	0.044

Signal ratio was calculated by dividing number of wells containing the active enzyme by number of wells analyzed.

Table S4. Summarized information about neurolysin signal ratio values for each patient with colorectal tumor and healthy control in the second set of experiments.

#	*Label*	*Stage*	*Neurolysin signal ratio (%)*
1	Colorectal tumor	I	0.196
2	Colorectal tumor	I	0.044
3	Colorectal tumor	I	0.097
4	Colorectal tumor	I	0.557
5	Colorectal tumor	I	0.370
6	Colorectal tumor	I	0.008
7	Colorectal tumor	I	0.073
8	Colorectal tumor	II A	0.057
9	Colorectal tumor	II A	0.036
10	Colorectal tumor	II A	0.023
11	Colorectal tumor	II A	0.047
12	Colorectal tumor	II A	0.295
13	Colorectal tumor	II A	0.591
14	Colorectal tumor	II A	0.059
15	Colorectal tumor	II A	0.011
16	Colorectal tumor	II A	0.138
17	Colorectal tumor	II A	0.120
18	Colorectal tumor	III	0.103
19	Colorectal tumor	III B	0.237
20	Colorectal tumor	III B	0.153
21	Colorectal tumor	III B	0.041
22	Colorectal tumor	III C	0.138
23	Colorectal tumor	III C	0.121
24	Colorectal tumor	IV B	0.067
25	Colorectal tumor	I	0.060
26	Colorectal tumor	I	0.025
27	Colorectal tumor	II A	0.909
28	Healthy	-	0.244
29	Healthy	-	0.128
30	Healthy	-	0.057
31	Healthy	-	0.035
32	Healthy	-	0.113
33	Healthy	-	0.108
34	Healthy	-	0.051
35	Healthy	-	0.022
36	Healthy	-	0.069
37	Healthy	-	0.033
38	Healthy	-	0.105
39	Healthy	-	0.012
40	Healthy	-	0.042
41	Healthy	-	0.039
42	Healthy	-	0.051
43	Healthy	-	0.129
44	Healthy	-	0.018
45	Healthy	-	0.013
46	Healthy	-	0.077
47	Healthy	-	0.095
48	Healthy	-	0.016
49	Healthy	-	0.050
50	Healthy	-	0.116
51	Healthy	-	0.028
52	Healthy	-	0.199
53	Healthy	-	0.034
54	Healthy	-	0.070
55	Healthy	-	0.010
56	Healthy	-	0.163
57	Healthy	-	0.025

Signal ratio was calculated by dividing number of wells containing the active enzyme by number of wells analyzed.

Table S5. The confusion matrix and evaluation metrics of neurolysin signal ratio test for colorectal tumor.

		Colorectal tumor	Healthy	total
Neurolysin signal ratio test (cut-off value = 0.052 %)	positive	23	9	32
	negative	5	21	26
	total	28	30	

Sensitivity = 0.82

Specificity = 0.70

Positive predictive value = 0.72

Negative predictive value = 0.81

[Comment] We decided the cut-off value at the closest point to the ideal upper left-hand corner **(Figure 4E)**[6]. According to the closest point to the upper left-hand corner, the cut-off value of the test was 0.052 %. At this point, the sensitivity and the specificity were 0.82 and 0.70, respectively. The positive predictive value and the negative predictive value were 0.72 and 0.81, respectively.

Table S6. The confusion matrix and evaluation metrics of neurolysin signal ratio test for colorectal tumor in the second set of experiments..

		Colorectal tumor	Healthy	total
Neurolysin signal ratio test (cut-off value = 0.057 %)	positive	19	13	32
	negative	8	17	25
	total	27	30	

Sensitivity = 0.70

Specificity = 0.57

Positive predictive value = 0.59

Negative predictive value = 0.68

[Comment] We decided the cut-off value at the closest point to the ideal upper left-hand corner (**Figure S15B),** in the same way as in **Table S5**. According to the closest point to the upper left-hand corner, the cut-off value of the test was 0.057 %. At this point, the sensitivity and the specificity were 0.70 and 0.57, respectively. The positive predictive value and the negative predictive value were 0.59 and 0.68, respectively.

Supplementary Figures

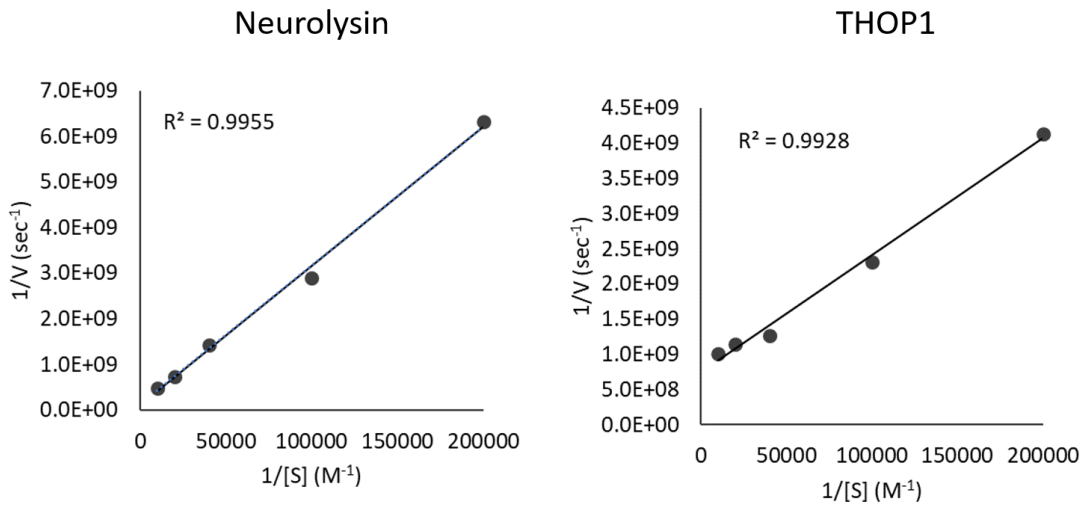

Figure S1. Lineweaver-Burk plot of LVVSTQTALA metabolism by recombinant neurolysin or THOP1 constructed from the same dataset as in **Figure 1C**.

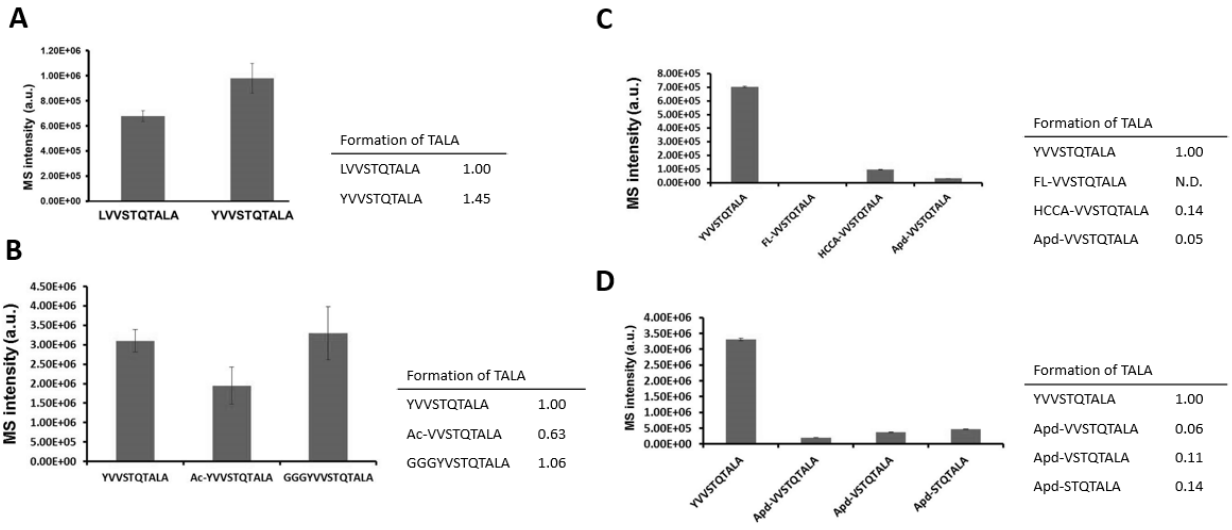

Figure S2. Comparison of N-terminal modified peptide reactivities toward neurolysin. For each experiment, the candidate peptide (10 μM) was mixed with recombinant neurolysin (0.36 μg/mL) and incubated for 4 h, and the formation of TALA peptide was monitored. Error bars represent S.E. (n = 3). (A) Comparison between LVVSTQTALA and YVVSTQTALA. (B) Analysis of the effects of N-terminal modification. (C) Analysis of the effects of N-terminal modification with fluorophores/quenchers. (D) Comparison of the reactivities of N-terminal Apd-modified peptides with different lengths.

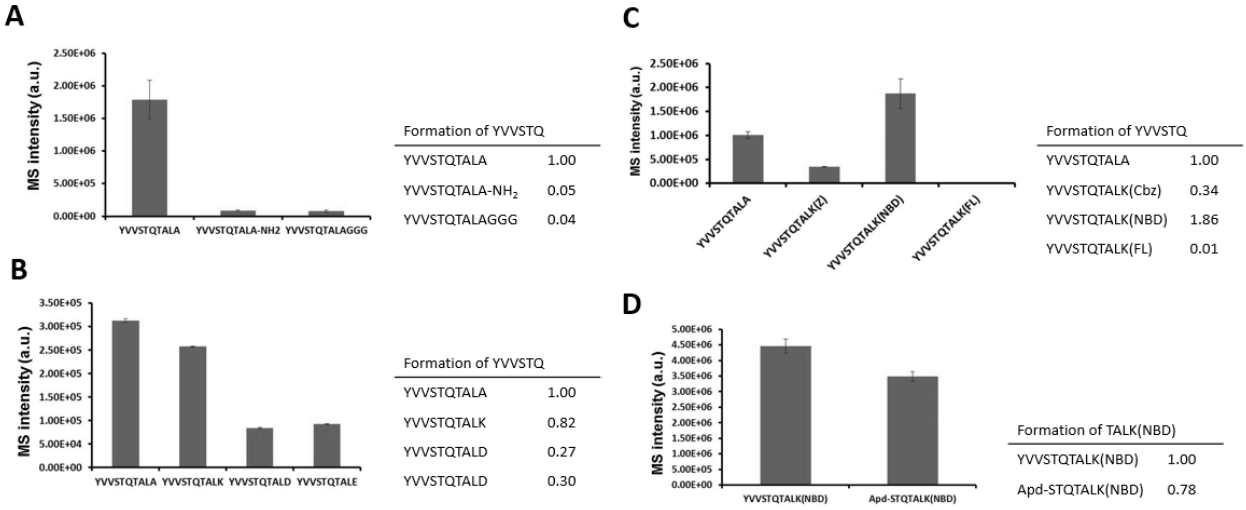

Figure S3. Comparison of reactivities of C-terminal modified peptides toward neurolysin. For each experiment, the candidate peptide (10 μM) was mixed with recombinant neurolysin (0.36 μg/mL) and incubated for 4 h, and the formation of YVVSTQ peptide was monitored. Error bars represent S.E. (n = 3). (A) Analysis of the effects of C-terminal modification. (B) Analysis of the C-terminal amino acid preferences. (C) Analysis of the effects of C-terminal side chain modification with fluorophores/quenchers. (D) Comparison of the reactivities of YVVSTQTALK(NBD) and Apd-STQTALK(NBD).

[Comment] A structure–activity relationship study was performed at several rounds (**Figure S2** and **S3**), and each round was performed using the YVVSTQTALA peptide as a standard. The peptides were designed to generate common products (TALA for C-terminus and YVSTQ for N-terminus) between entries, and the amount of products was compared to estimate the relative reaction speed of the peptide for neurolysin.

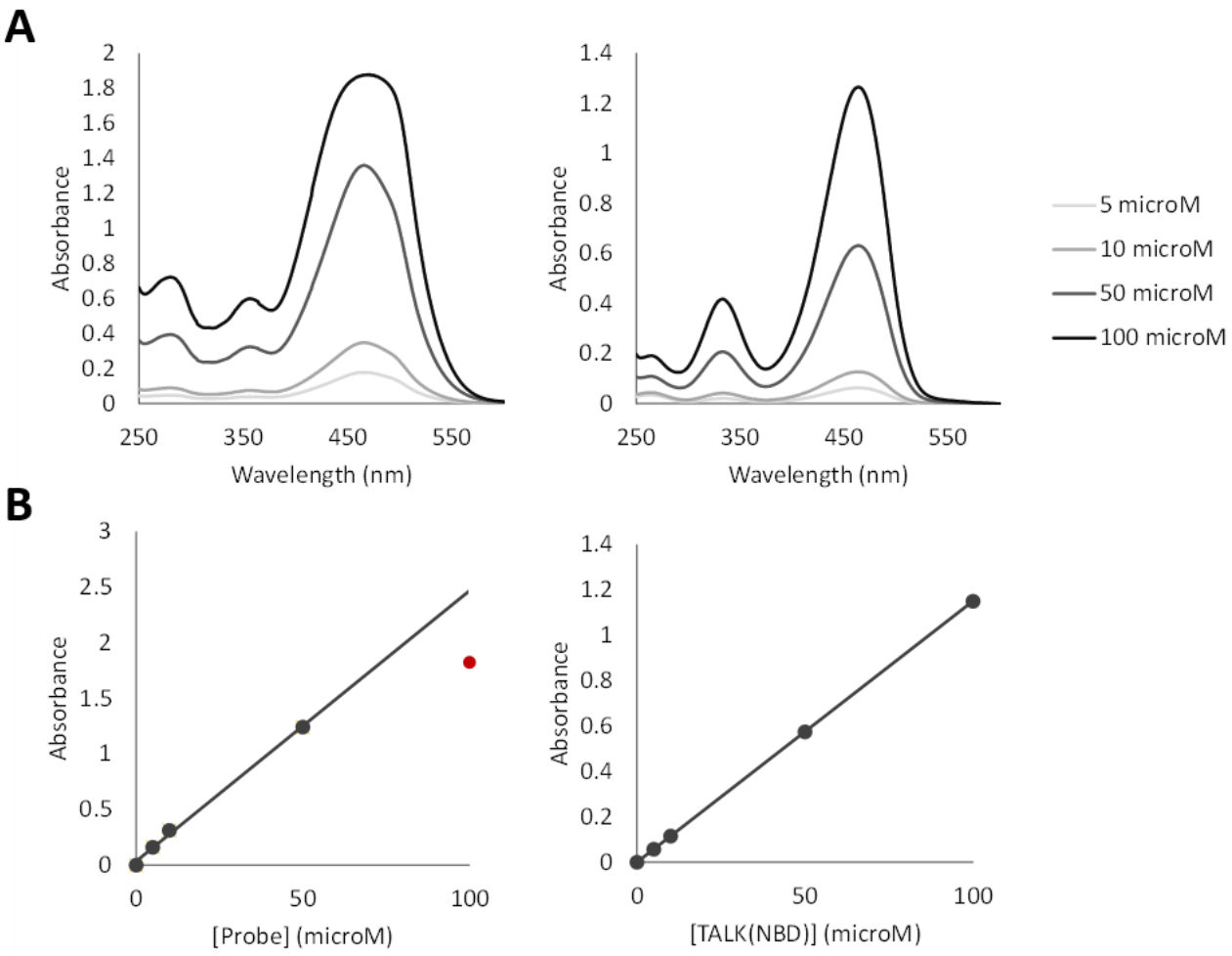

Figure S4. (A) Concentration-dependent absorbance spectra of the probe (Apd-STQTALK(NBD), left) and the fluorescent product (TALK(NBD), right) in phosphate-buffered saline (PBS, pH 7.4). (B) 450 nm absorbance of the probe (left) and the fluorescent product (right) plotted against concentrations.

[Comment] 450 nm absorbance of the probe (Apd-STQTALK(NBD)) linearly increased upon increased concentration to up to 50 μM. At 100 μM, absorbance spectra showed the irregular shape (**Figure S4A** left) and lost the linearity (**Figure S4B** left, red dot), indicating that the probe was not diffusely soluble and generated the precipitates or aggregation. From this data, we concluded that the probe is sufficiently soluble to concentration at 50 μM or less.

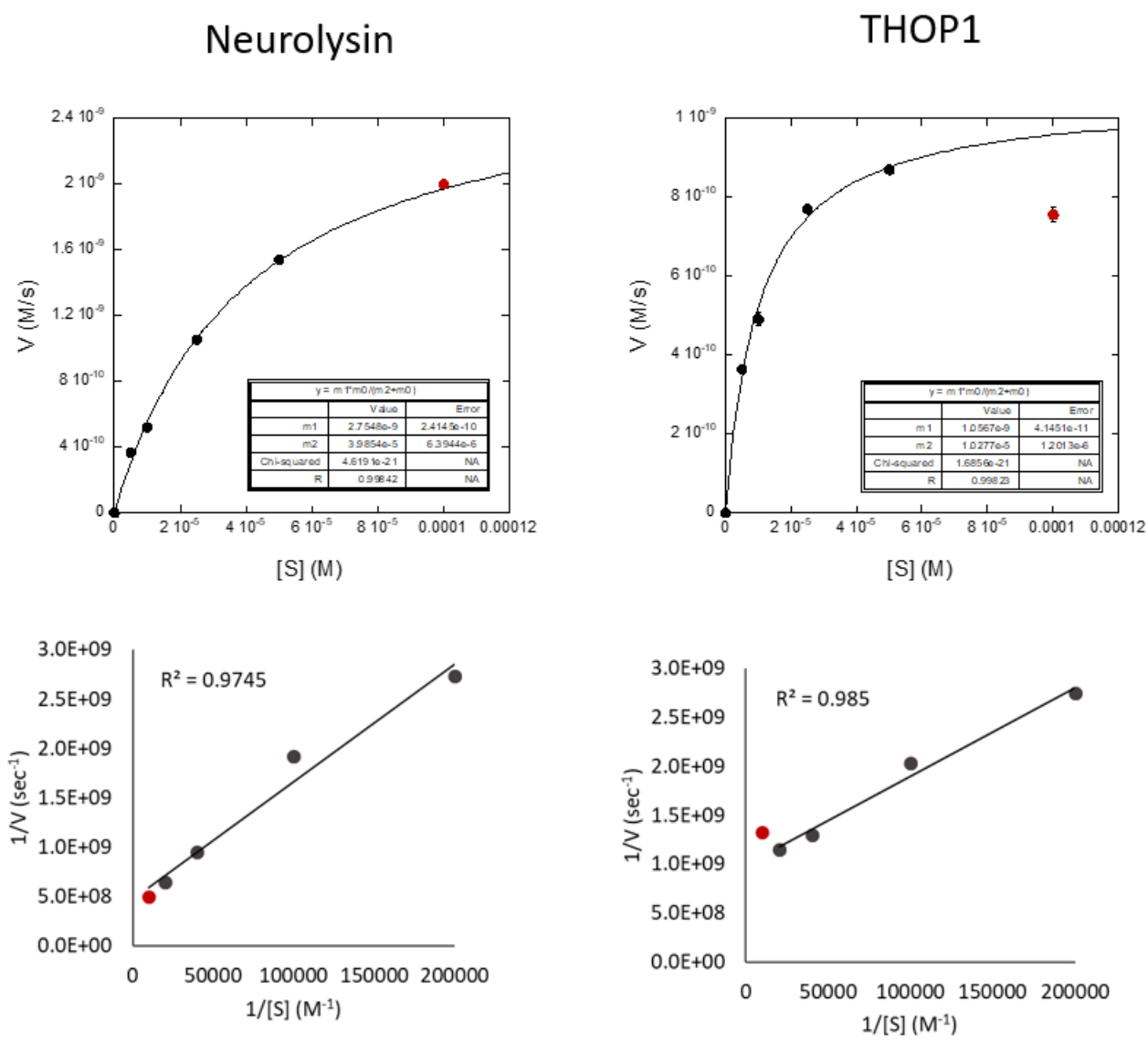

Figure S5. Michaelis–Menten plot (top) and Lineweaver-Burk plot (bottom) of Apd-STQTALK(NBD) metabolism by recombinant neurolysin (left) or THOP1 (right) (1 μg/mL). Error bars represent S.E. (n = 3). k_{cat} and K_m values were determined based on non-linear regression using the equation shown in the graph. Data point at 100 μM (shown in red dot), in which the probe was not sufficiently soluble, was not included in the fitting.

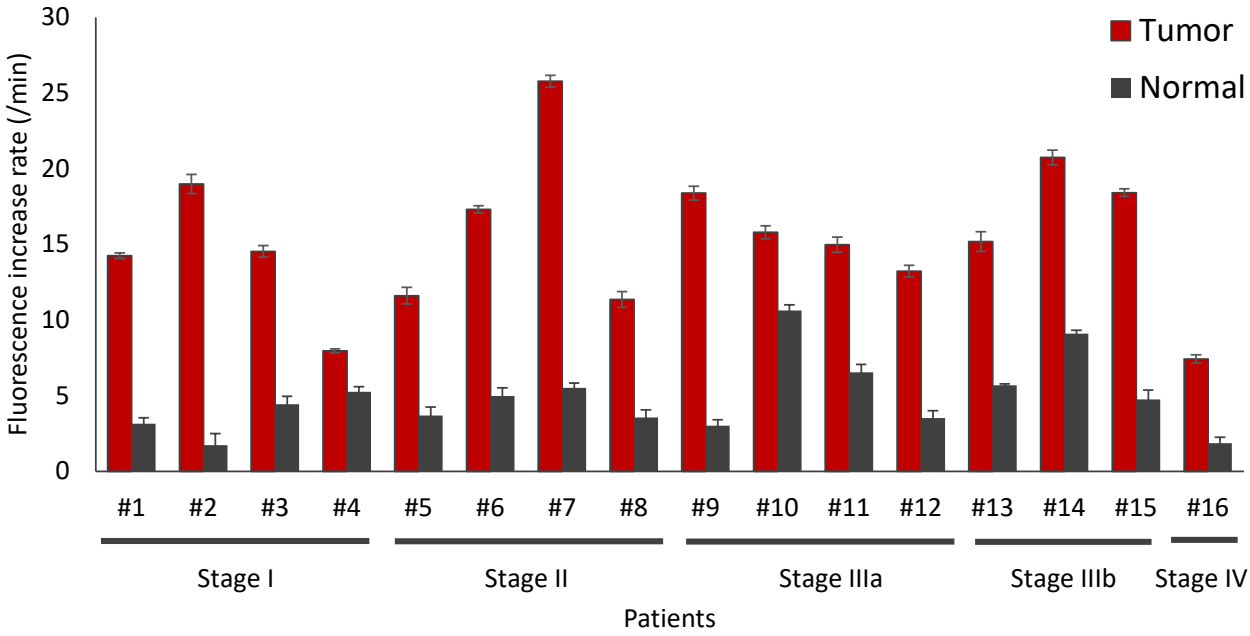

Figure S6. Fluorescence increases of Apd-STQTALK(NBD) (10 μM) after mixing with tumor and non-tumor tissue lysate (0.02 mg/mL) from colorectal tumor surgical specimen for 30 min. The samples were derived from 16 patients as a pair of tumor and non-tumor tissues. The tumor stages are shown below the number of patients. Error bars represent S.E. (n = 4).

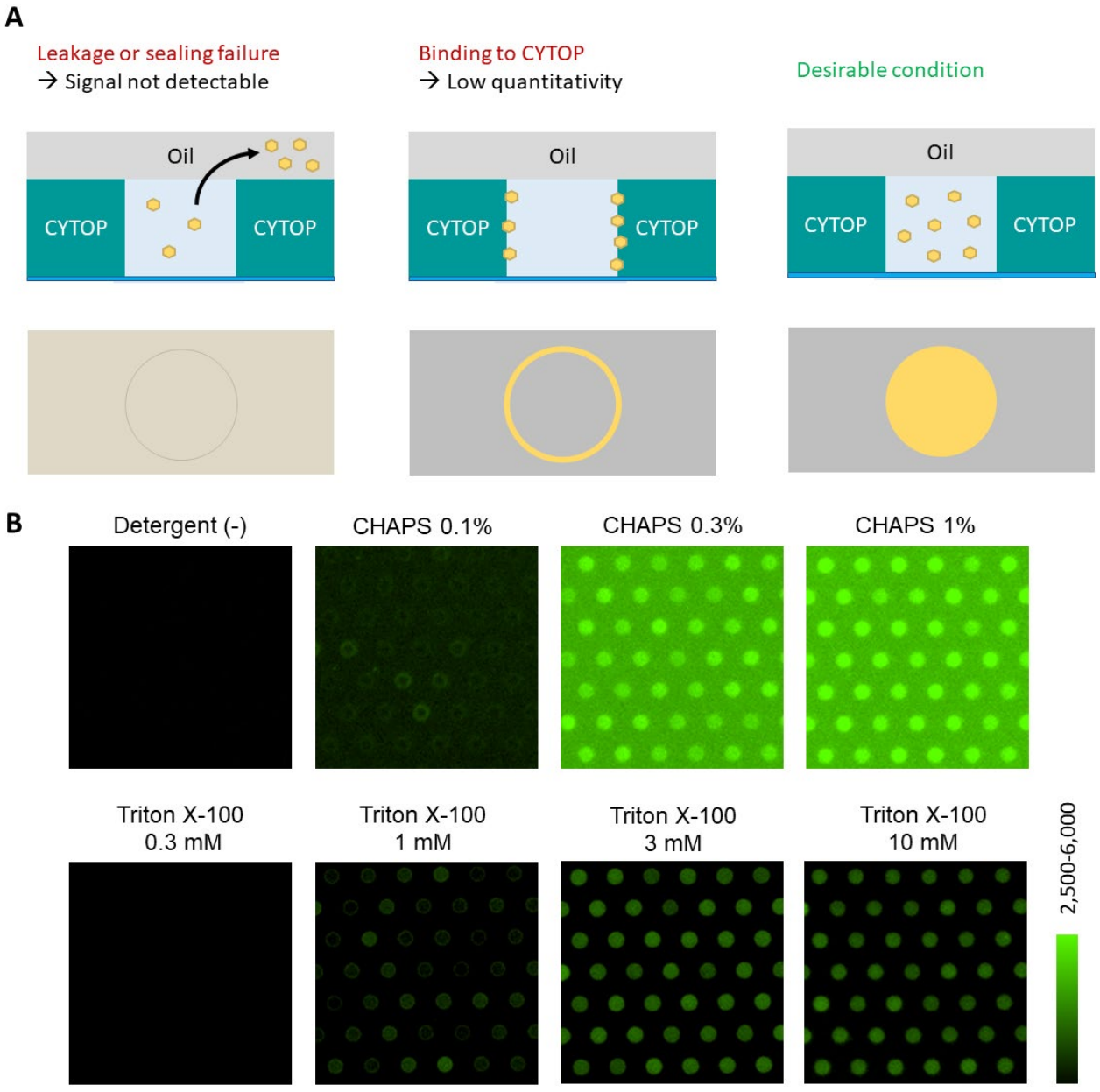

Figure S7. (A) Requirement of adequate conditions in single-molecule enzyme activity analysis. Top = vertical cut image of the chamber. Yellow hexagonal structures indicate the probes. Bottom = expected fluorescence images in each condition. (B) Fluorescence images of the microdevices after loading probes (50 μM) and recombinant neurolysin (100 ng/mL) in HEPES buffer (pH 7.4) containing CHAPS (0.1-1%) or Triton X-100 (0.3-10 mM).

[Comment] We optimized assay conditions so that we can uniformly load the FRET-based peptidase probes in the microchambers. When the concentration of the detergent was too low, the fluorescence signal was not monitorable since the probe solution was not adequately loaded or the sealing by oil was not sufficient. At higher concentrations of detergents, fluorescent spots were detected, but it showed the circled fluorescence signals surrounding the chamber (as seen in CHAPS 0.1% and Triton X-100 1 mM), which was an indication of the non-specific binding of the probes to the inner walls of the chamber. High

concentration of CHAPS yielded the fluorescence signals detected outside of the chambers (as seen in CHAPS 0.3% and 1%). Among the conditions we tested, use of 3 mM Triton X-100 exhibited the best signal-to-background ratio, and we decided it to be the optimal detergent concentrations.

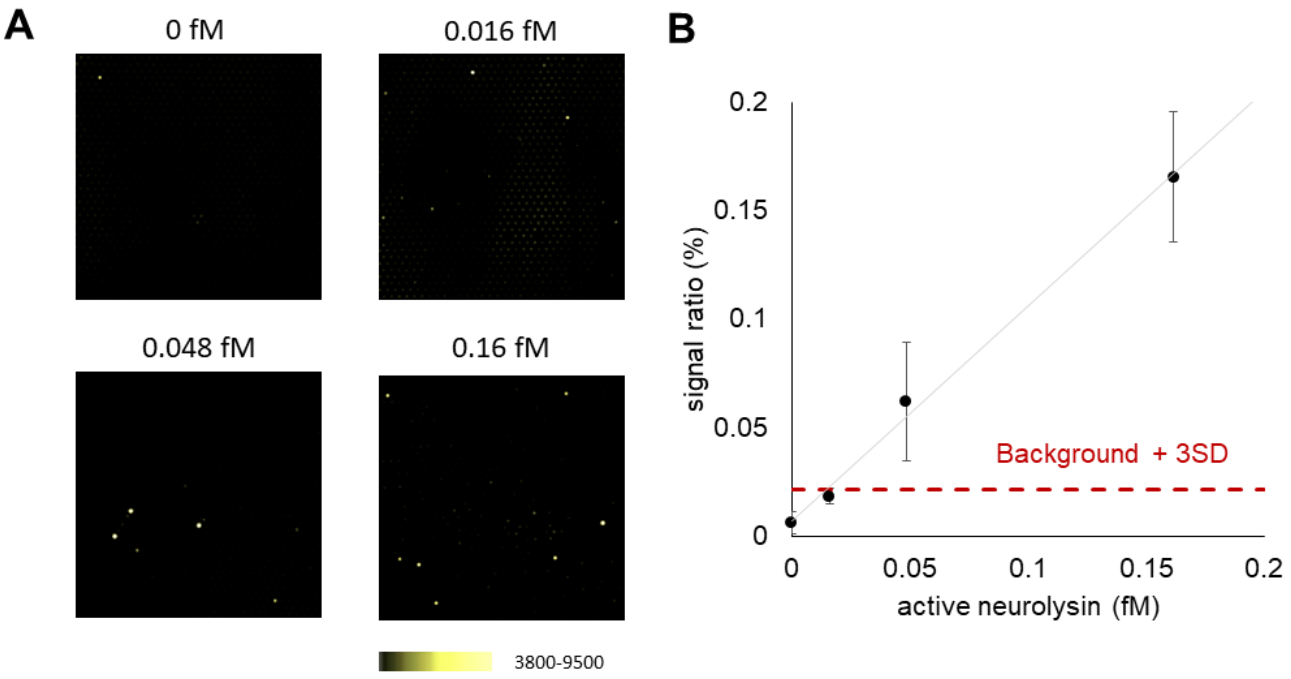

Figure. S8. Detection limit of active neurolysin in microdevice-based assay. (A) Fluorescence images of the microdevices containing active neurolysin (calculated concentrations of active enzymes were 0, 0.016, 0.048, and 0.16 fM) with Apd-STQTALK(NBD) (50 μM), after incubation for 4 h. (B) The signal ratio versus active recombinant neurolysin concentration. The error bars represent S.D. (n = 3), and the red line represents the signal ratio of the background under recombinant neurolysin-free condition plus 3 times the S.D.

[Comment] We calculated the observed lambda value (microchamber with the fluorescence signal/total microchamber analysed) in the analysis of 100 ng/mL recombinant neurolysin to be 1.65×10^{-3}. The observed lambda was less than that expected from the loaded recombinant enzyme (when the molecular weight of neurolysin was 78,000, the expected lambda was 13.1 for 100 ng/mL). The detection limit of the active neurolysin concentration was calculated based on the counting of the number of spots containing the active enzymes.

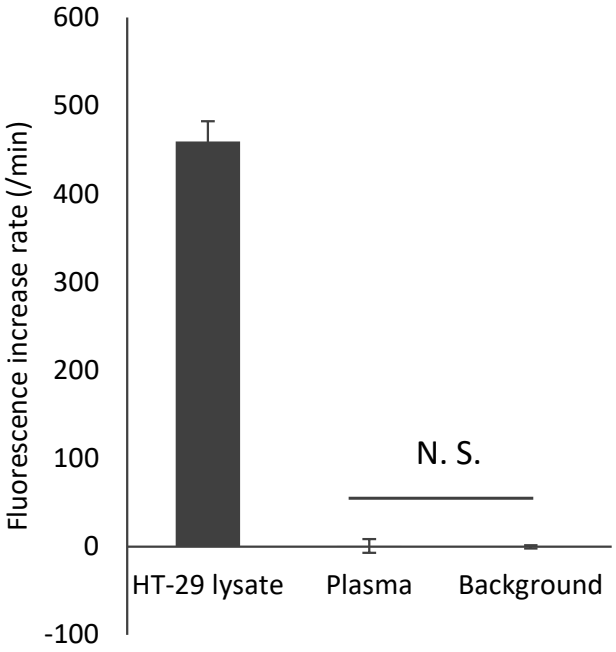

Figure S9. Detection of neuropeptidase activity using the conventional assay with the microplate reader. Cell lysate of HT-29 colorectal tumor cells (0.1 mg/mL) or plasma samples of healthy subjects (0.1 mg/mL) were mixed with Apd-STQTALK(NBD) (10 μM) in DPBS (pH 7.4) containing 0.1 % CHAPS and incubated in 384-well plate for 1 h at 37 °C. Fluorescence signals were monitored every 2 min using microplate reader, and the slope of the fluorescence increase was calculated. Error bars represent S. D. (n = 6). N. S. indicates that the value was not significant (p = 0.47, Student's t-test).

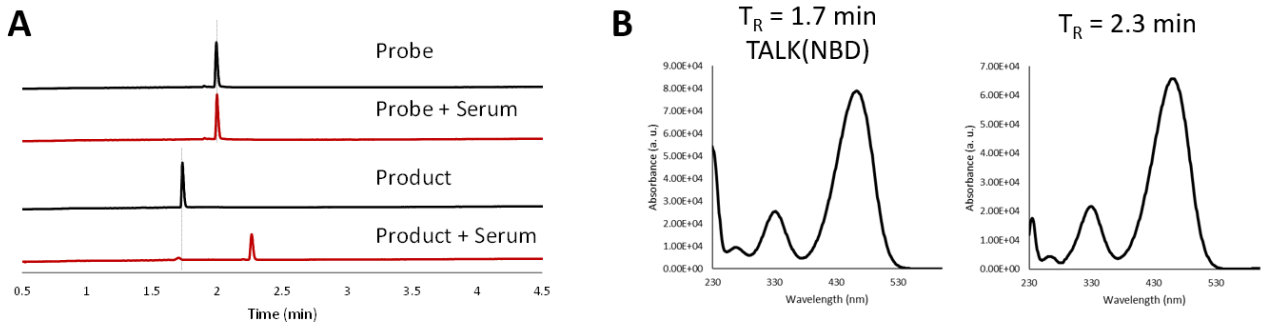

Figure S10. Stability of probe (Apd-STQTALK(NBD)) and product (TALK(NBD)) (100 μM) in 1/10-diluted human serum in PBS (pH 7.4) containing 0.1% CHAPS for 18 h at room temperature. (A) Absorbance chromatograms (monitored at 450 nm) of the samples. The sample treated without serum (black line) or with serum (red line) were compared, and the peak height was normalized to that without serum. (B) Absorbance spectra in the analysis of product (TALK (NBD), T_R = 1.7 min) and the new product generated in the serum (T_R = 2.3 min).

[Comment] We attempted to use the probe to detect the activity of neuropeptidases in plasma samples using the conventional microplate reader-based assay (**Figure S9**), but an increase of fluorescence signal was not detected in the standard assay protocol. Under the same conditions, the activity of neuropeptidase in the cell lysate of HT-29 colorectal tumor cells was detected, indicating that the amount of active neuropeptidases in plasma samples is much lower than that detectable in cell or tissue lysates. The result was confirmed by LC-MS/MS-based analysis (**Figure S10A**, top). After incubating the probe (Apd-STQTALK(NBD)) with 1/10-diluted serum, the formation of product TALK(NBD) was hardly detectable in absorbance chromatogram. In the same assay, the stability of the estimated product TALK(NBD) was also monitored (**Figure S10A**, bottom). In this, (1) formation of new product (R_T = 2.3 min), and (2) slight decrease of overall 450 nm absorbance, were observed. As for (1), we consider that the free N-terminus of TALK(NBD) was metabolized by aminopeptidases present in serum. The mass number of the peak was not identified, but it retained the absorbance of NBD (**Figure S10B**, left), so it is expected to be fluorescently active. As for (2), the result indicated that NBD fluorophore is not completely stable in serum, but the single-molecule assay is performed in the diluted conditions (1/500) and under the separation of the proteins in the microchamber, and we consider that the effect is not as problematical as that of the assay performed in the mixture.

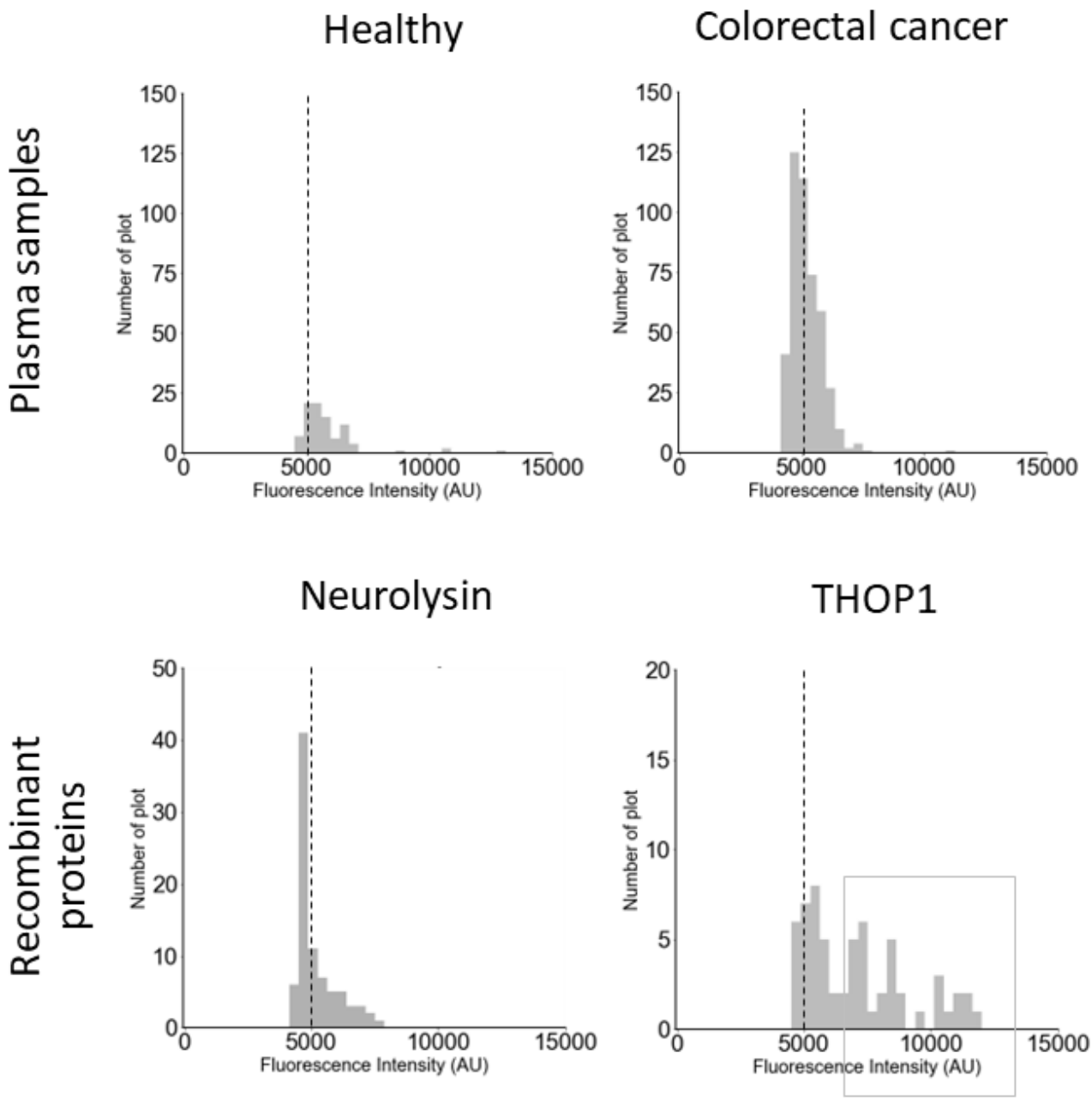

Figure S11. Activity histograms of human plasma samples (1/500 dilution) and recombinant enzymes (neurolysin and THOP1, 100 ng/mL). The fluorescence intensities of the observed spots in the single-molecule analysis were plotted.

[Comment] In the single-molecule activity histogram, fluorescence signals in plasma samples were detected at positions comparable to those observed for recombinant neurolysin. The signal intensity of recombinant THOP1 ranged from approximately 4,600–12,000, whereas in human plasma, fluorescence spots with a signal stronger than 8,000 were barely detected. From these results, we consider that the major enzymes detected in plasma samples were likely due to neurolysin rather than THOP1.

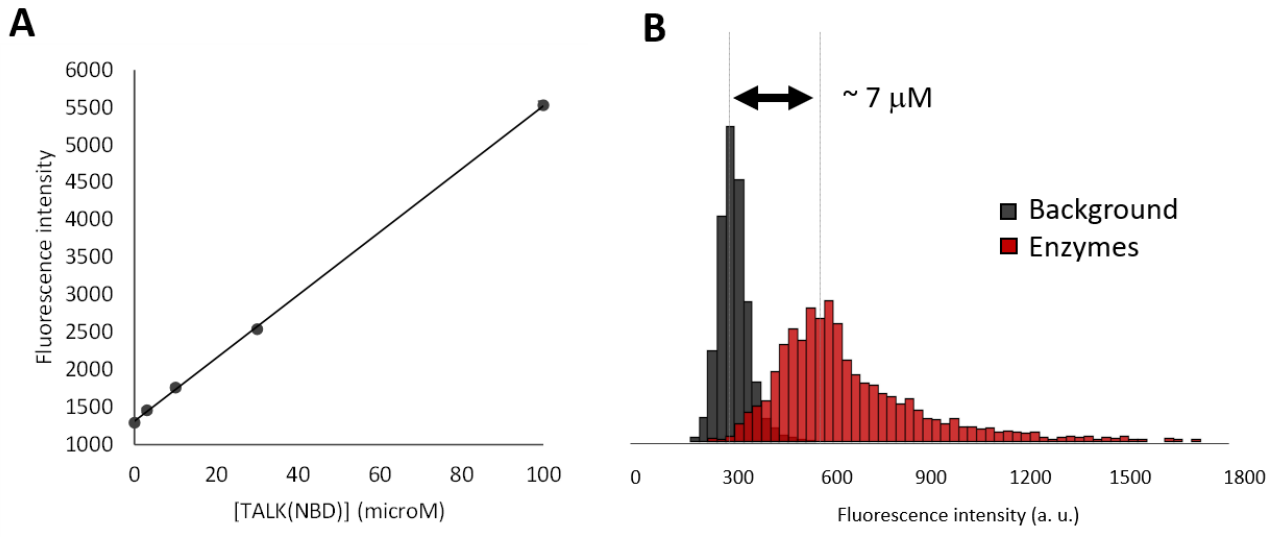

Figure S12. (A) Confirmation of the linearity of fluorescence intensities of TALK(NBD) in the microdevice. Varied concentrations of TALK(NBD) was dissolved in PBS (pH 7.4) containing Triton X-100 (3 mM) and loaded into microdevice, and the fluorescence images were taken. The average intensities of the wells were calculated, and plotted against the concentration of NBD(TALK) loaded. (B) Histogram of the activity analysis in microdevices for plasma samples from colorectal tumor patients (1/500 dilution) with Apd-STQTALK(NBD) (50 μM), after incubation at 37˚C for 4 h. The condition of fluorescence microscopy was same as in (A). First 10,000 wells (most of which were assigned as empty wells) were quantified to make a histogram of background (black), and wells assigned to contain enzymes were quantified to make a histogram of enzymes (red). The gap of the fluorescence intensities of the peak tops were converted to estimated concentration of TALK(NBD) generated in the chamber.

[Comment] Due to the limited solubility of the probe, the concentration of the probe used in the assay (50 μM) was around K_m for neurolysin (**Figure S5**), so the velocity of enzymatic reaction was not close to V_{max} and was subject to the decrease of probe concentration [S] by metabolic consumption. The approximate amount of probes reacted in the chamber was estimated to be around 7 μM using the calibration curve generated in **Figure S12A**, indicating that less than 20% of probes were consumed in most wells containing the enzyme

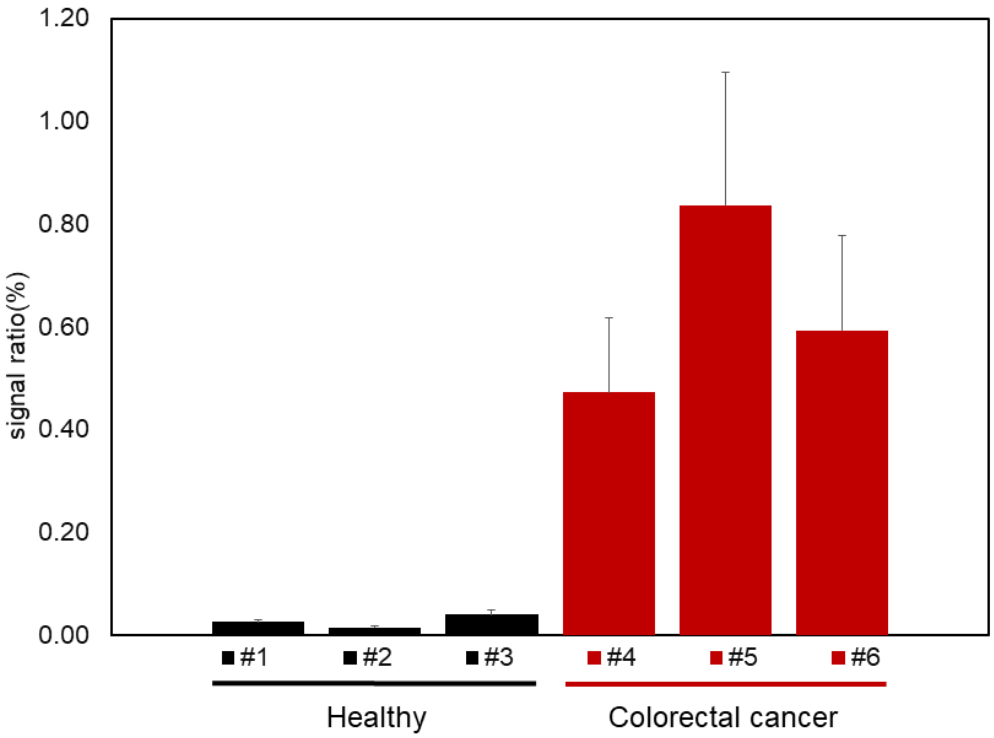

Figure S13. Validation analysis for detected signals in microdevice-based assay. The bar chart represents the signal ratio of three patients with colorectal cancer and three healthy individuals. The error bars represent S.E.M (n = 3).

[Comment] To confirm the assay results and to support the discovery that neuropeptidase activities were elevated in certain classes of patients with colorectal tumor, we picked up three patients who showed elevated enzyme counts and compared the results with three randomly selected healthy subjects, and repeated the activity analysis. The validation experiments were performed in triplicate, and this tendency was confirmed.

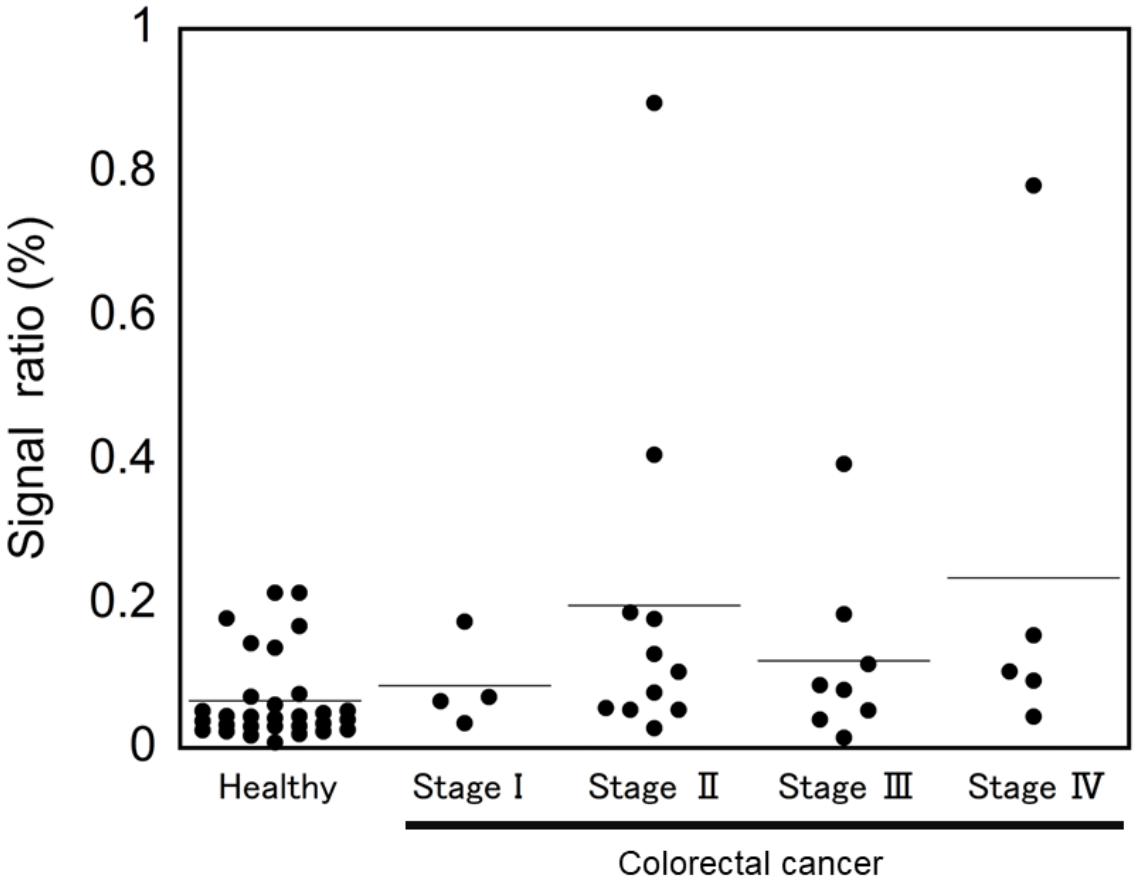

Figure S14. The dot-plot diagram of the signal ratio value in each plasma sample for healthy and each colorectal cancer stage (I, II, III and IV).

[Comment] We discovered that some patients showed the elevated signal ratio in blood samples in stage II, III, and IV, and that the signal ratio was not necessarily elevated as their stage advanced.

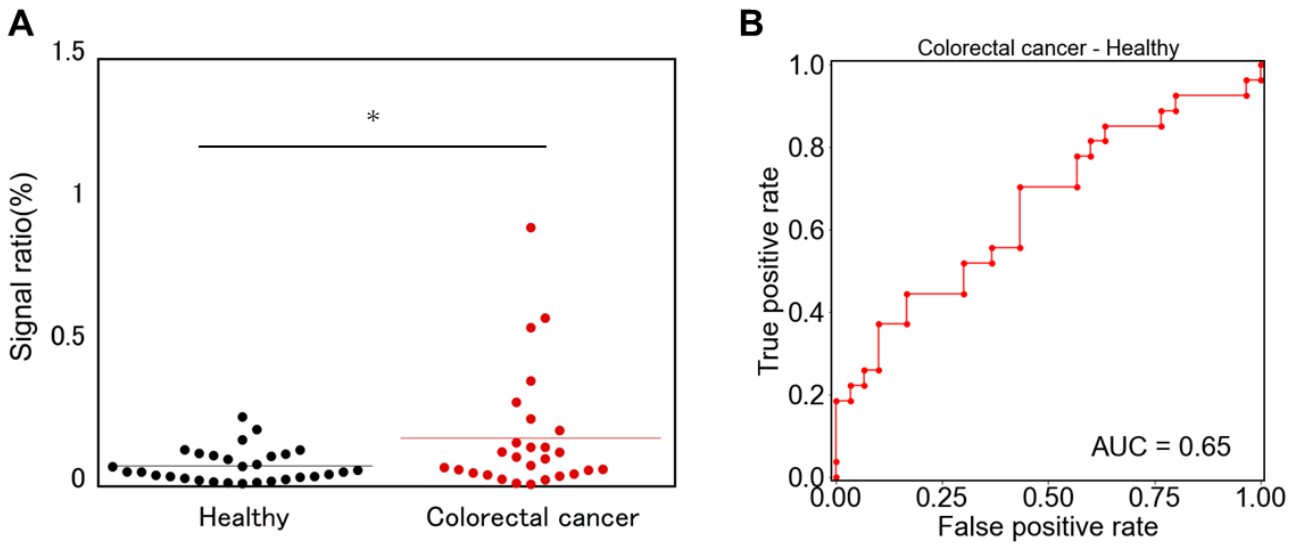

Figure S15. Validation analysis for detected signals in another sample groups. The assay was performed with blood samples of 30 healthy subjects and 27 patients with colorectal tumors that were collected independently from those used in **Figure 4D**. The assays were performed in double-blind conditions. (A) The dot-plot diagram of the signal ratio value in each plasma sample (*p < 0.05, Mann-Whitney U test). (B) Receiver operating characteristic (ROC) curve and AUC value for diagnosis of patients with colorectal cancer. The ROC curve was calculated from the number of detected points for patients with colorectal cancer versus healthy subjects.

[Comment] In the second set of samples, AUC = 0.65 was obtained, and was lower than AUC = 0.75 in the first set of samples. We consider that the variation of AUC between the study originated from that we were treating only small number of patient groups, but in both studies, the trend was repeated that subclass of patients with high neurolysin activity was observed in patients with colorectal tumor (**Figure 4D** and **S15A**).

Supplementary references

1 J. Onagi, T. Komatsu, Y. Ichihashi, Y. Kuriki, M. Kamiya, T. Terai, T. Ueno, K. Hanaoka, H. Matsuzaki, K. Hata, T. Watanabe, T. Nagano and Y. Urano, *J Am Chem Soc*, 2017, **139**, 3465–3472.

2 K. Honda, Y. Hayashida, T. Umaki, T. Okusaka, T. Kosuge, S. Kikuchi, M. Endo, A. Tsuchida, T. Aoki, T. Itoi, F. Moriyasu, S. Hirohashi and T. Yamada, *Cancer Res*, 2005, **65**, 10613–10622.

3 K. Honda, T. Okusaka, K. Felix, S. Nakamori, N. Sata, H. Nagai, T. Ioka, A. Tsuchida, T. Shimahara, M. Shimahara, Y. Yasunami, H. Kuwabara, T. Sakuma, Y. Otsuka, N. Ota, M. Shitashige, T. Kosuge, M. W. Büchler and T. Yamada, *PLoS One*, 2012, **7**, e46908.

4 H. Shinoda, Y. Taguchi, R. Nakagawa, A. Makino, S. Okazaki, M. Nakano, Y. Muramoto, C. Takahashi, I. Takahashi, J. Ando, T. Noda, O. Nureki, H. Nishimasu and R. Watanabe, *Commun Biol*, 2021, **4**, 476.

5 S. Sakamoto, T. Komatsu, R. Watanabe, Y. Zhang, T. Inoue, M. Kawaguchi, H. Nakagawa, T. Ueno, T. Okusaka, K. Honda, H. Noji and Y. Urano, *Sci Adv*, 2020, **6**, eaay0888.

6 A. K. Akobeng, *Acta Paediatrica, International Journal of Paediatrics*, 2007, **96**, 644–647.